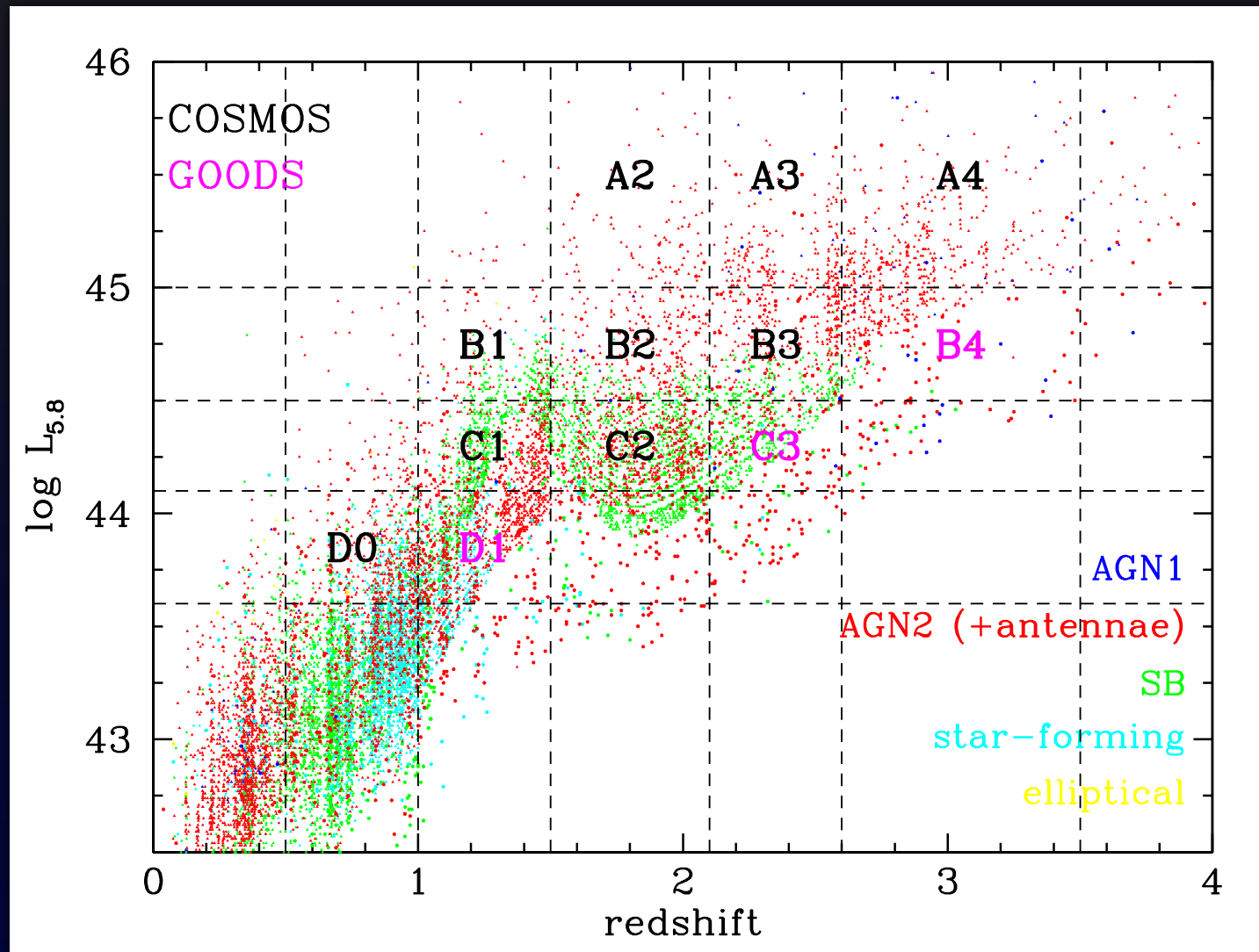


The (mid-IR) sample

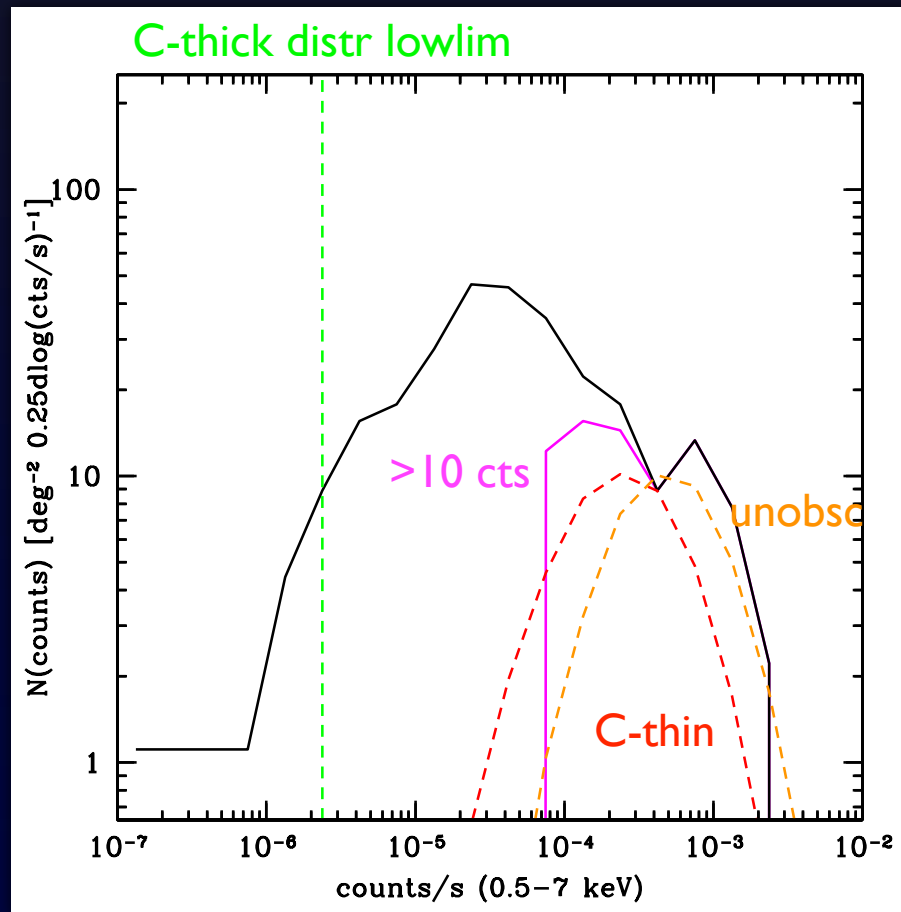


>16000 24 um selected sources

X-ray count rate distribution

We generated the expected count rate distributions of unabsorbed, C-thin & C-thick AGN as predicted from the La Franca+05 luminosity function, assuming a scaling relation between 5.8 μm and X-ray luminosities and an average X-ray spectrum (function of N_{H}).

All 24 μm galaxies: without using any color/SED selection



By comparing the expected and observed count rate distributions we define (for each bin) a count rate range in which we perform the following stacking analysis and simulations.

unobscured: $20 < \log N_{\text{H}} < 22$

Compton-thin: $22 < \log N_{\text{H}} < 24$

Compton-thick: $24 < \log N_{\text{H}} < 25$

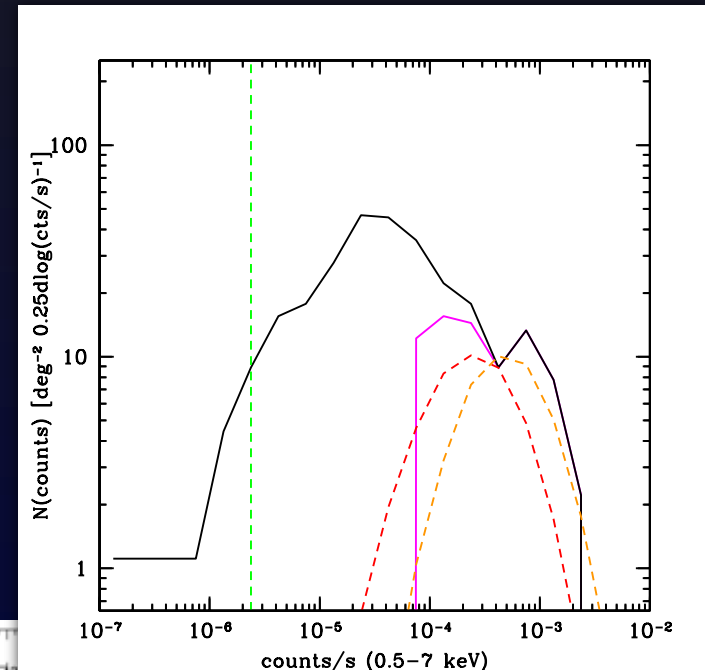
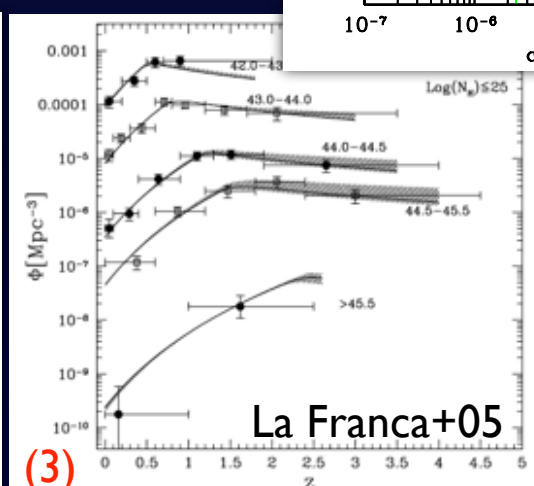
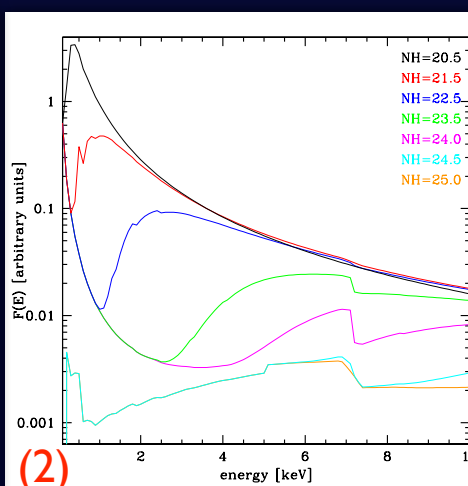
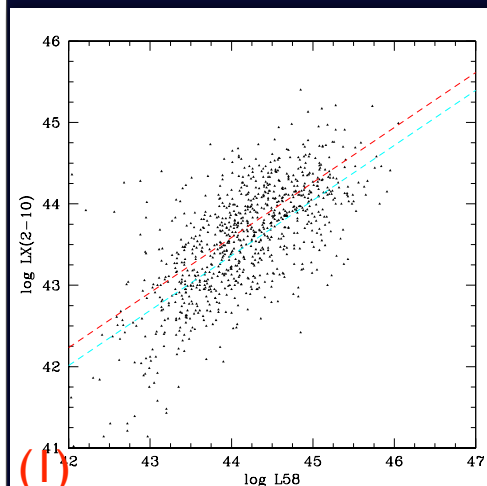
X-ray undetected sources

We searched for Compton-thick AGN among 24 μm sources below the X-ray detection limit. In order to select samples of candidate Compton-thick, an efficient selection criterion is needed.

New technique: comparison between observed X-ray count rate distributions (of 24 μm sources) and expectations obtained through simulations.

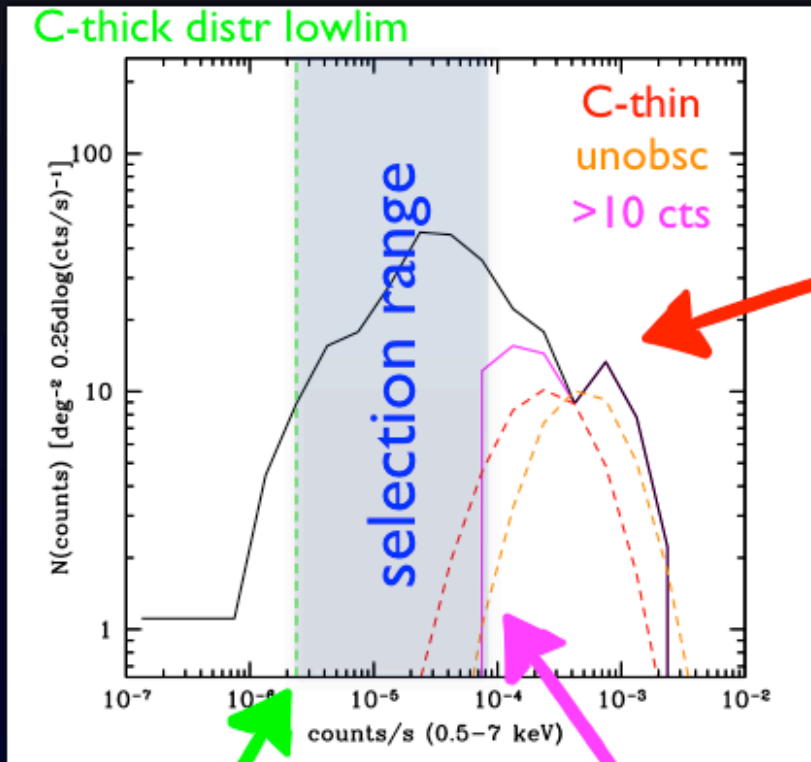
Ingredients:

- (1) L58-LX relation
- (2) average spectral shape
- (3) X-ray luminosity function

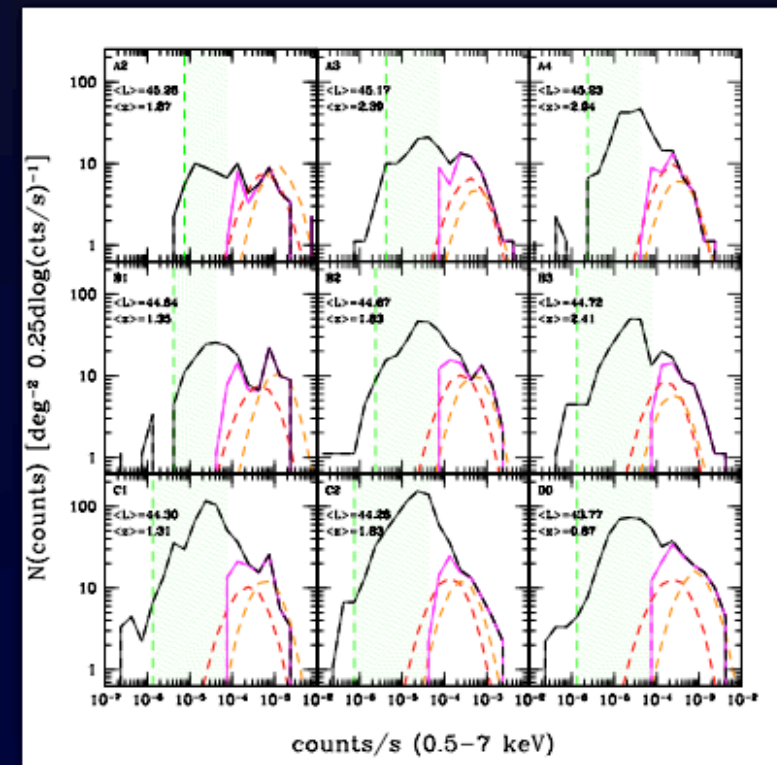


X-ray count rate distribution

This is not a color or a SED selection



good agreement between the expected unobscured & C-thin AGN distributions and the secondary peak observed at high count rates.

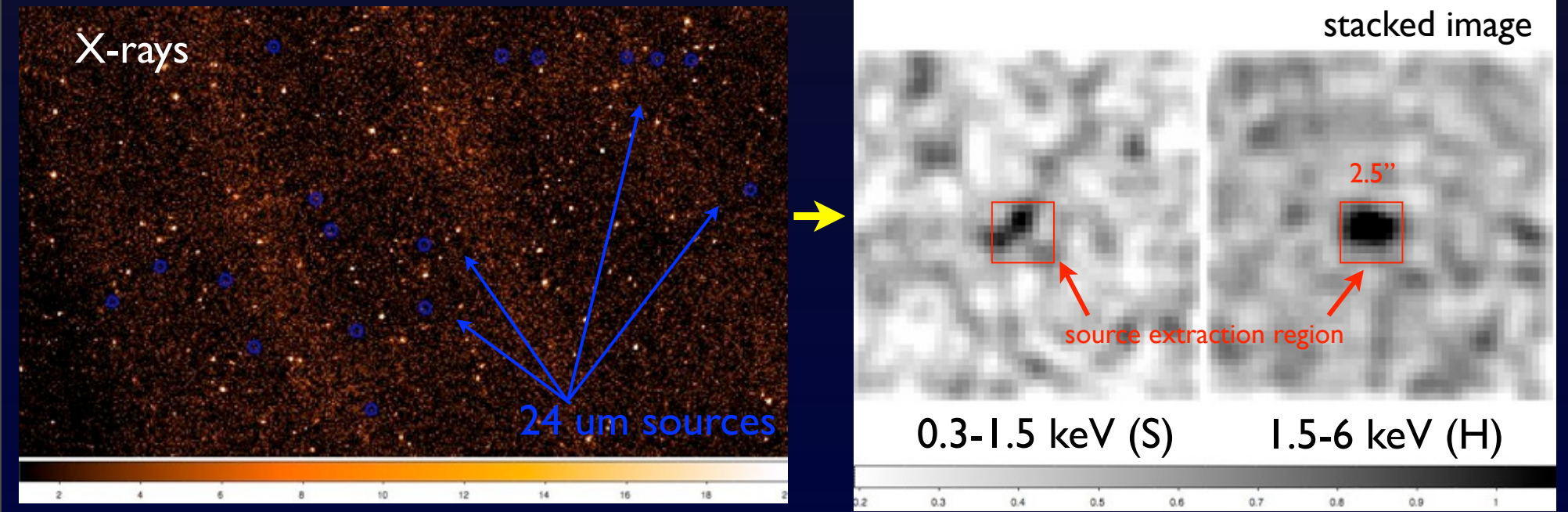


Stacking analysis

The X-ray counts in the positions of the MIR sources (without detection!) are summed together: increase in effective exposure time and decrease in flux limit.

Stacking in two bands: soft (0.3-1.5 keV) and hard (1.5-6) to evaluate the mean hardness ratio for the selected candidates.

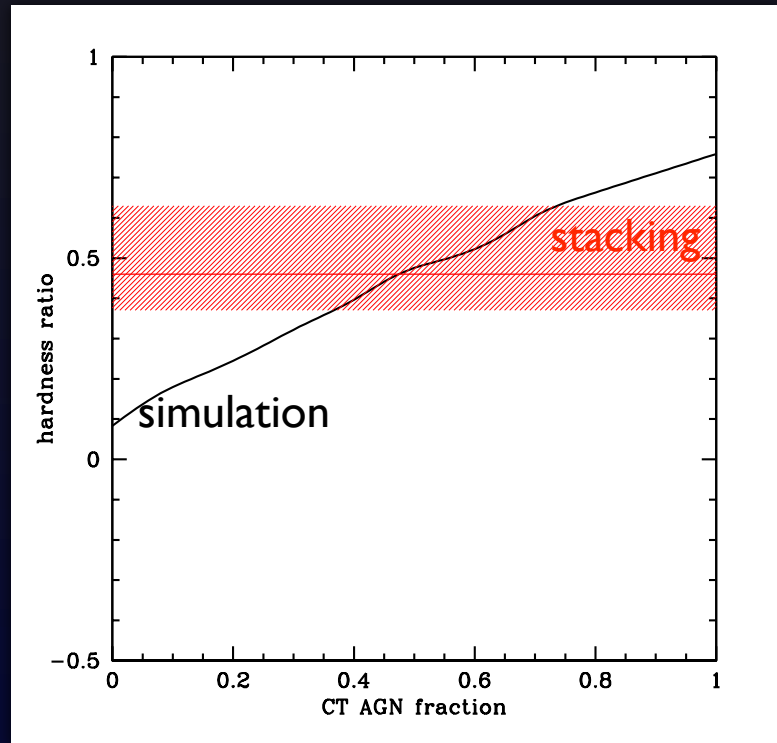
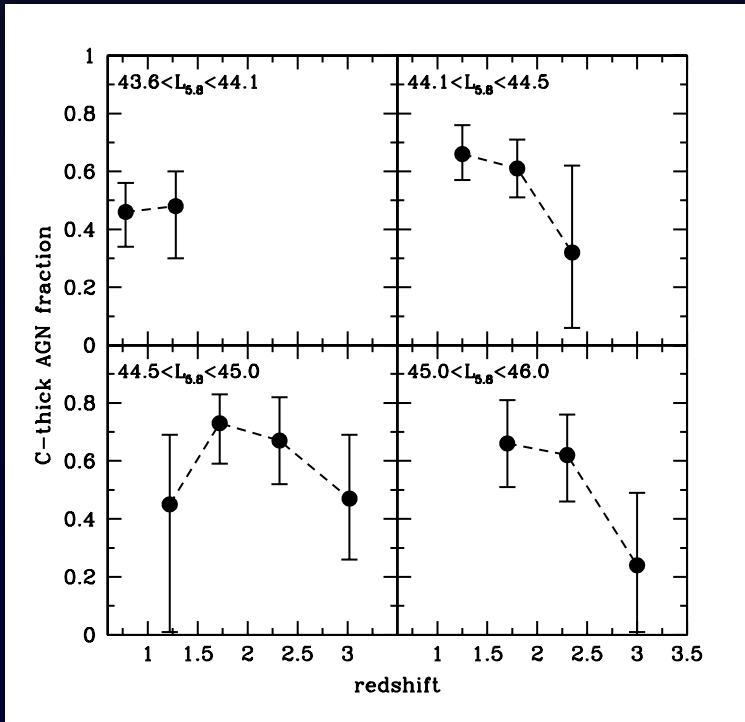
$HR = (H-S)/(H+S)$ related to the spectral shape -> measure of the obscuration



From HR to C-thick fraction

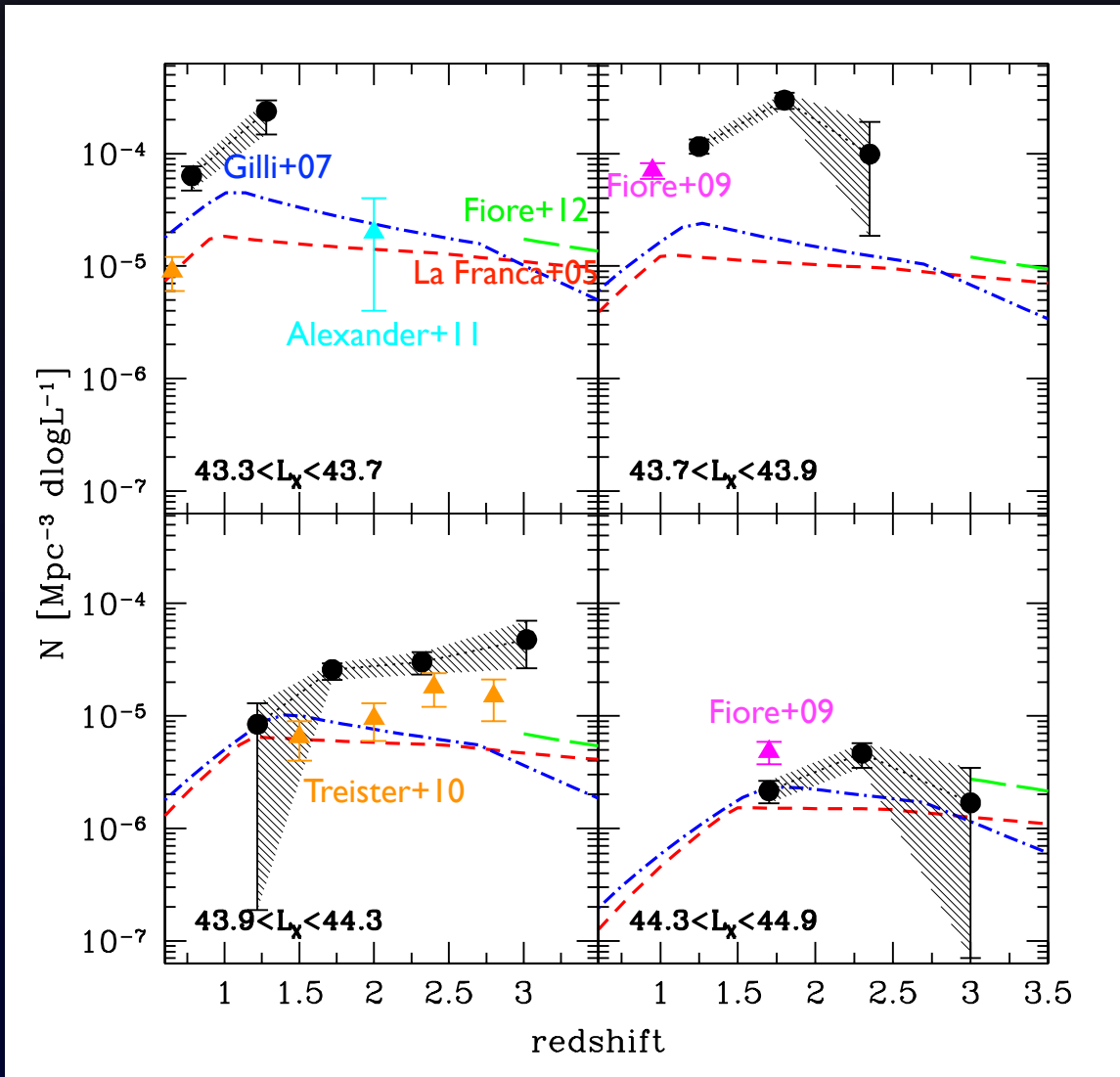
HR values obtained from stacking analysis are converted in fractions of C-thick AGN using Monte Carlo simulations.

In each bin we computed the average HR as a function of the fraction of C-thick AGN (assuming that the sources are either C-thick AGN or SF galaxies).



The comparison between observed and simulated HR allowed us to constrain the C-thick AGN fraction in each bin.

CT volume density



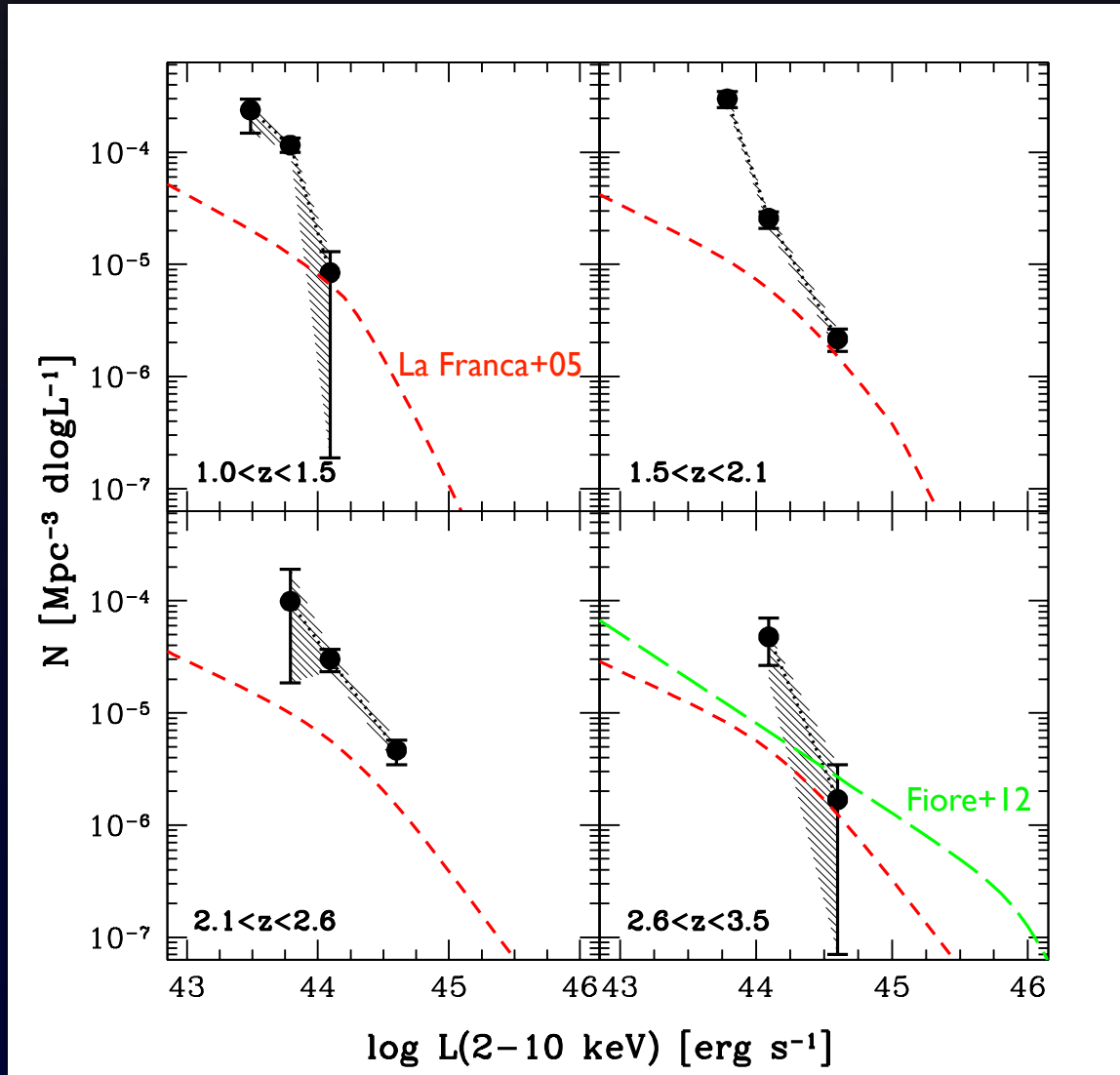
We corrected in each bin the density of MIR sources by the fraction of C-thick AGN.

The contribution of detected C-thick AGN from Brightman&Ueda12 has been included.

Fair agreement with model expectations at high L ($>10^{44}$ erg/s).

At $L \sim 10^{43}$ erg/s we found density up to 10 times higher than predicted.

CT volume density



At $L \sim 10^{43} \text{ erg/s}$ we found density up to 10 times higher than predicted (in good agreement with other estimates, e.g. Fiore +09)

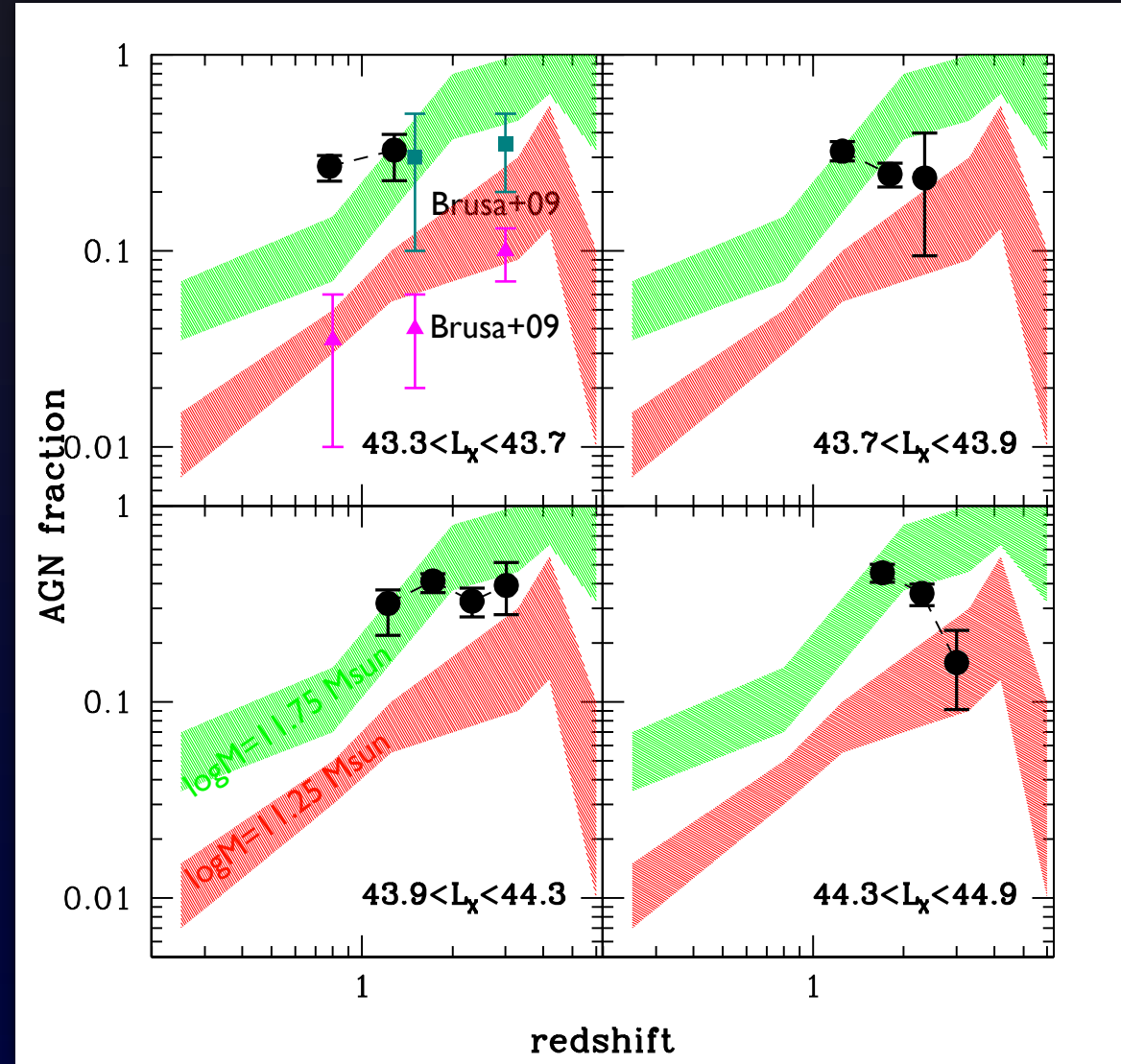
Downsizing trend (as observed in C-thin AGN).

Total accreted BH mass still in agreement with local estimates:

$$\rho_{BH} = 3.55 \times 10^5 M_\odot \text{ Mpc}^{-3}$$

(unobscured + C-thin + C-thick)

AGN duty cycle



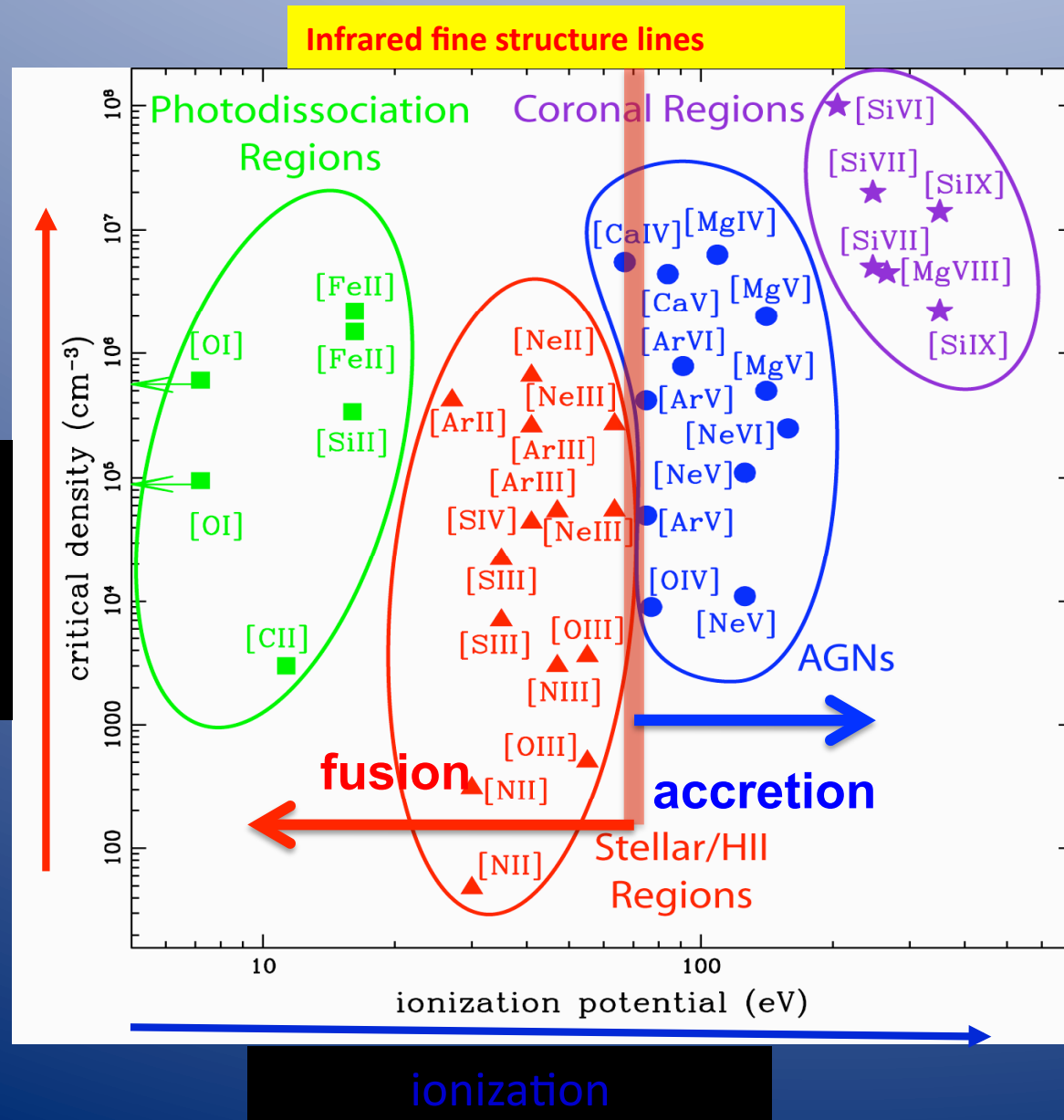
Def: fraction of AGN over all galaxies with same mass.

Different models of AGN triggering predict different redshift evolution of the duty cycle.

We found an almost constant value ($\sim 30\%$) at high z.

shaded areas: Fiore+12

How to separate star formation and accretion with infrared spectroscopy

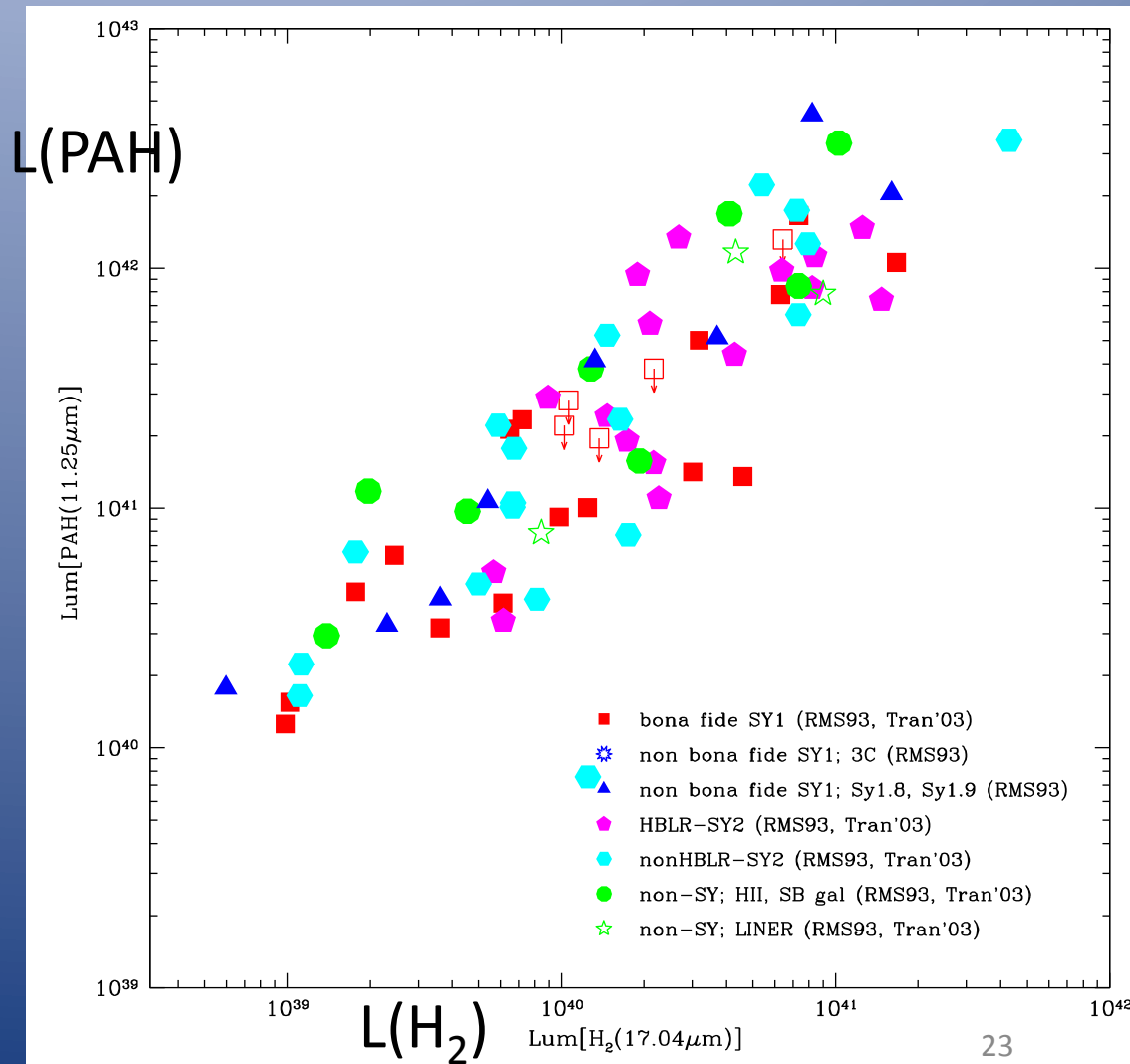


IR fine structure lines:

- separate different physical mechanisms,
- cover the ionization-density parameter space
- do not suffer heavily from extinction

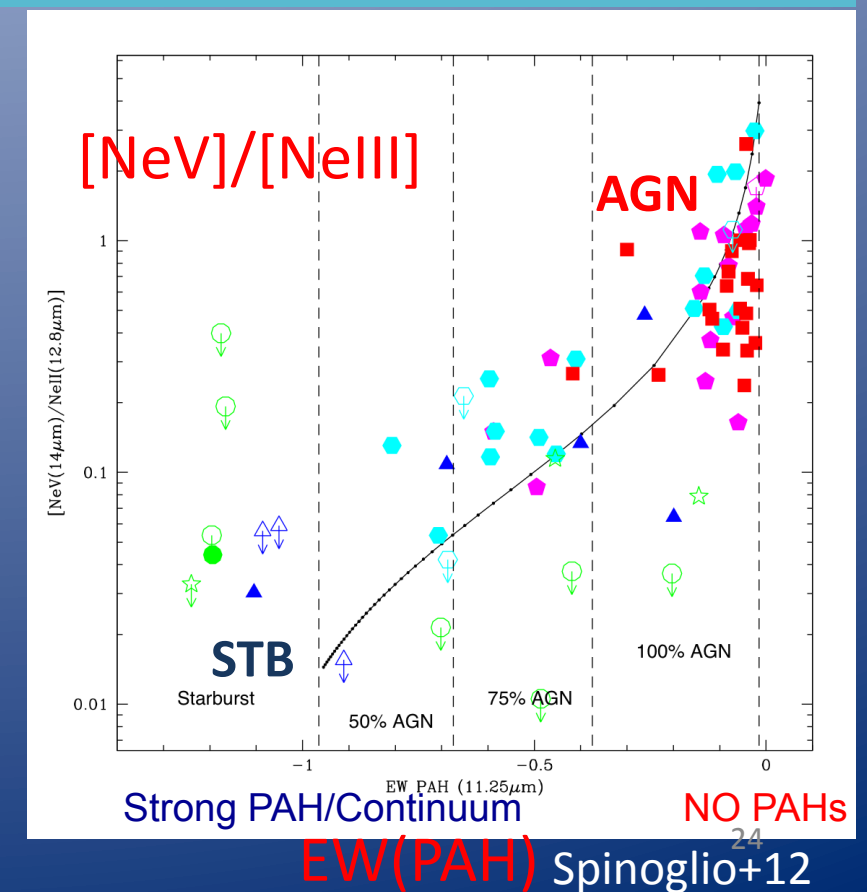
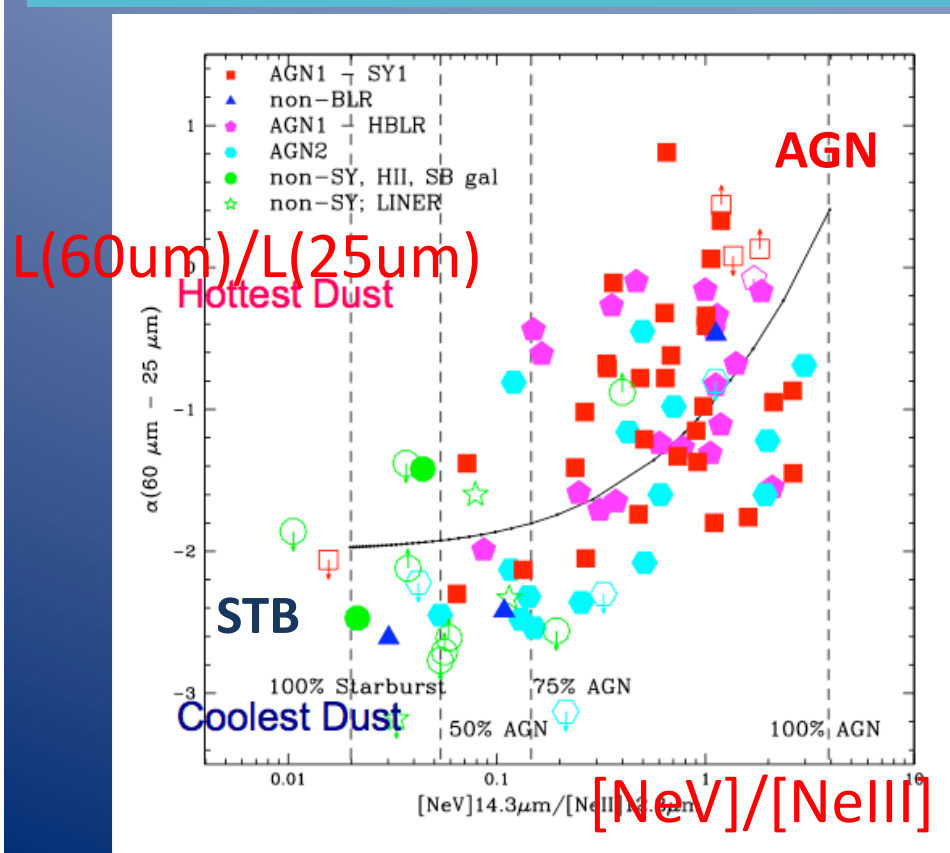
Mid-IR contains several new candidates for Star Formation Rate indicators

- Traditionally, take H recombination line, since each recombination corresponds to one photo-ionization
- [N II] 12.8 μm forbidden line
- [S III] 34 μm forbidden line
- [Si II] 35 μm forbidden line
- ... (extended 25 μm continuum)
- PAH features (eg 11.25 μm) or LIR???
- H₂ emission lines (eg. 17.04 μm)??



AGN/Starburst Mixing Diagrams comparing Lines and Continua

- Seyfert 1's (red) and Seyfert 2's with Polarized Broad Lines (magenta) have mid-IR emission dominated by AGN, in contrast to starbursts and LINERs (green). Seyfert 2's without Polarized Broad Lines (cyan) are a mixed bag. Some probably have their central AGN shut down currently (i.e. this century).
- These ionization-sensitive []-line ratios tell the same story as the IR dust continuum: a stronger AGN contribution is closely tied to stronger (nonstellar) 12 — 25 μm continuum from hot dust near the nucleus, with NO PAH's.



AGN diagnostic diagrams: model

Semi-analytical models
to disentangle the AGN and Starburst contribution
to the total galaxy emission

Expression of the

PAH11.25 μm EW
[NeV]14.32 μm /[Nell]
[OIV]/[Nell]
[Nell] EW
Extendedness
 $\alpha_{(60-25)\mu\text{m}}$

as functions of R

$$R = F_{19\mu\text{m}}^{\text{gal}} / F_{19\mu\text{m}}^{\text{AGN}}$$

Theoretically for each of the galaxies there are 6 R_i
→ if at least 3 of them are consistent with each other
→ reliable $\langle R \rangle$ is computed
→ the AGN percentage in that galaxy is estimated.

[NeV] as indicator of AGN activity

The [NeV] emission lines is a basic requirement

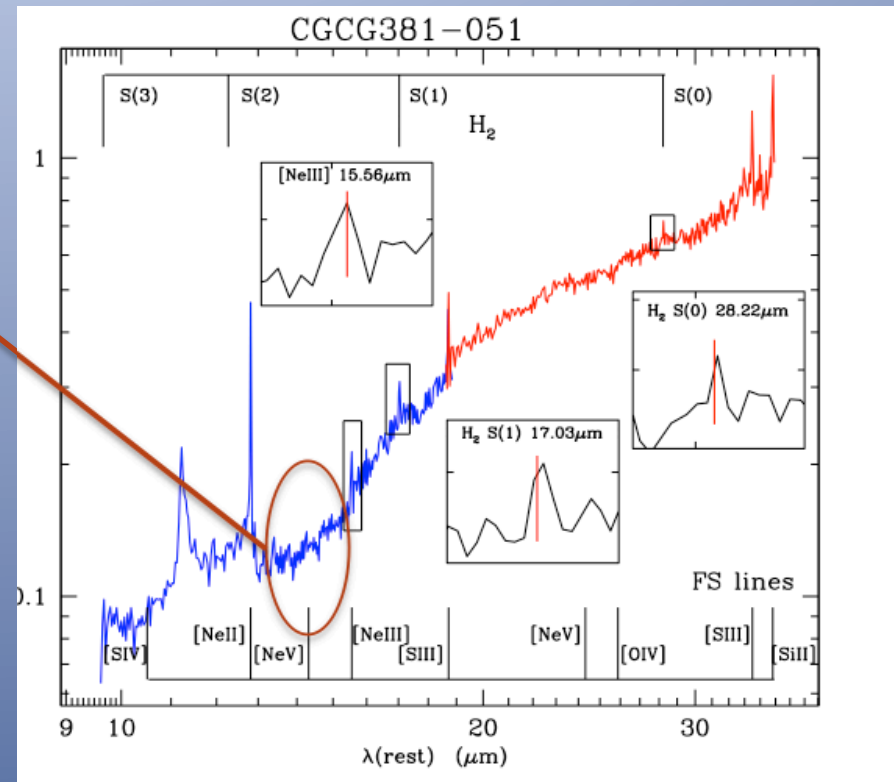
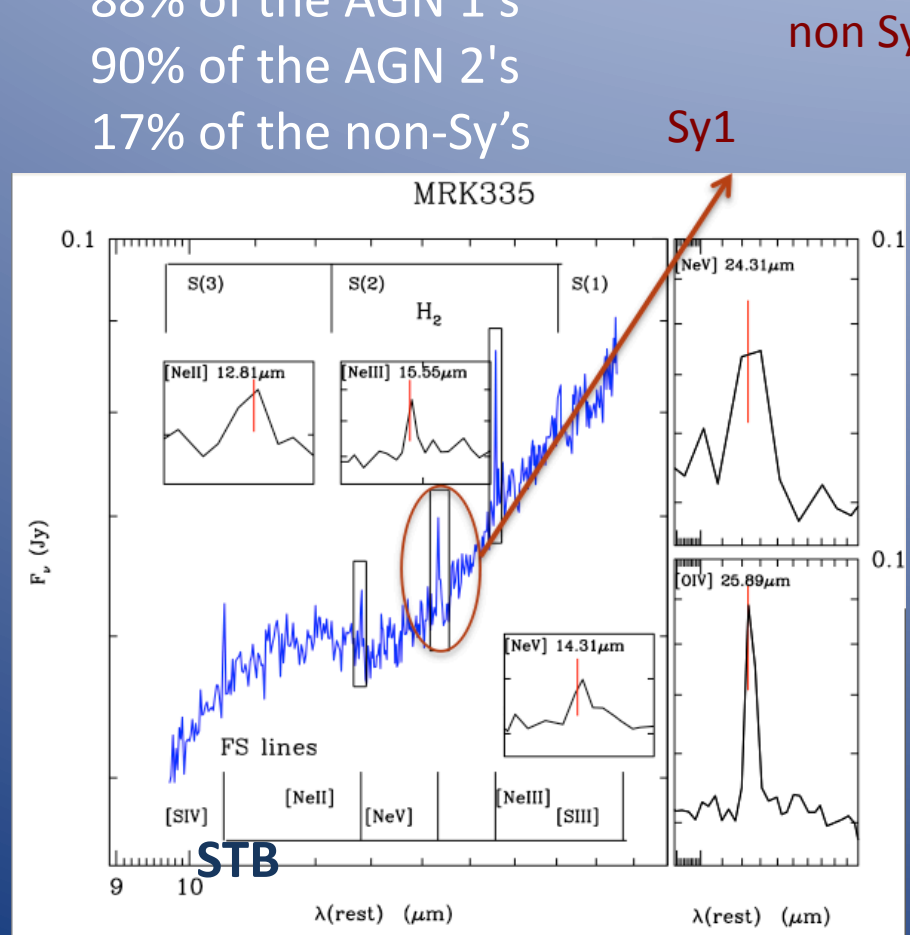
for a galaxy to be classified as an AGN:

It is detected in the

88% of the AGN 1's

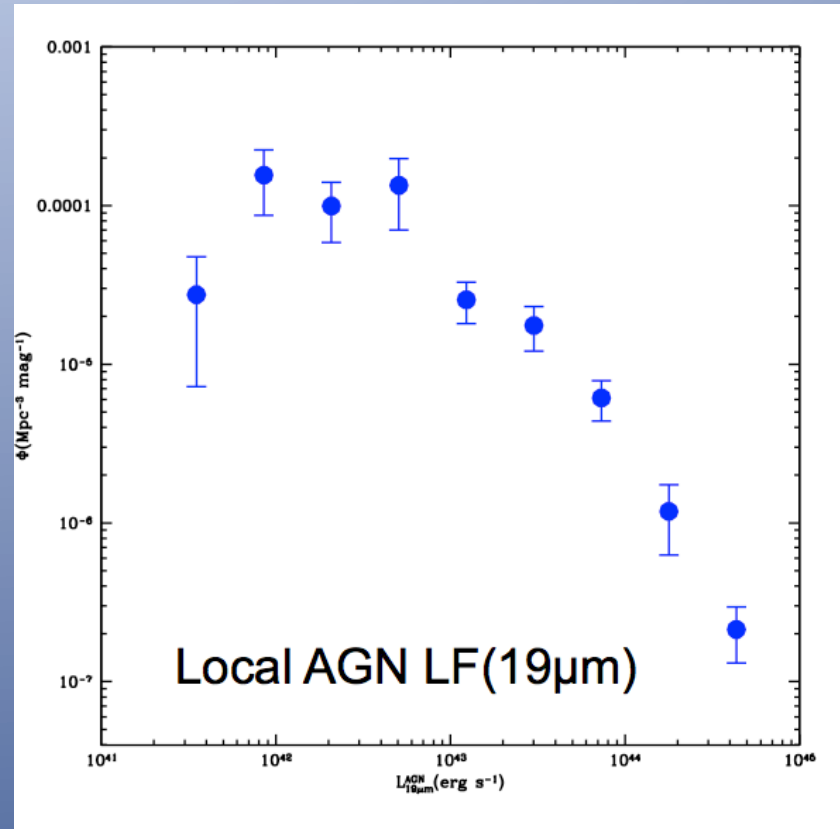
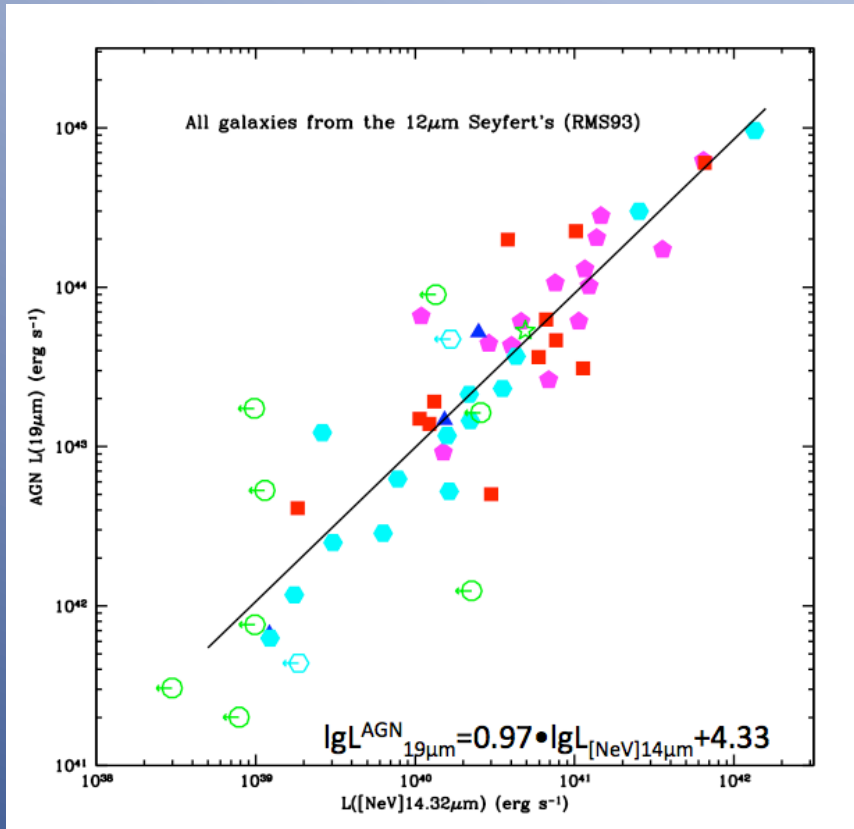
90% of the AGN 2's

17% of the non-Sy's



Deep spectroscopic searches for
[NeV] lines
can discover relatively weaker AGN with
lower luminosities.
(cf. Goulding & Alexander 09)

AGN statistics: AGN power



AGN fractional luminosity @19μm
vs [NeV]14.3μm line luminosity

[Nell] as Star Formation index, same approach →

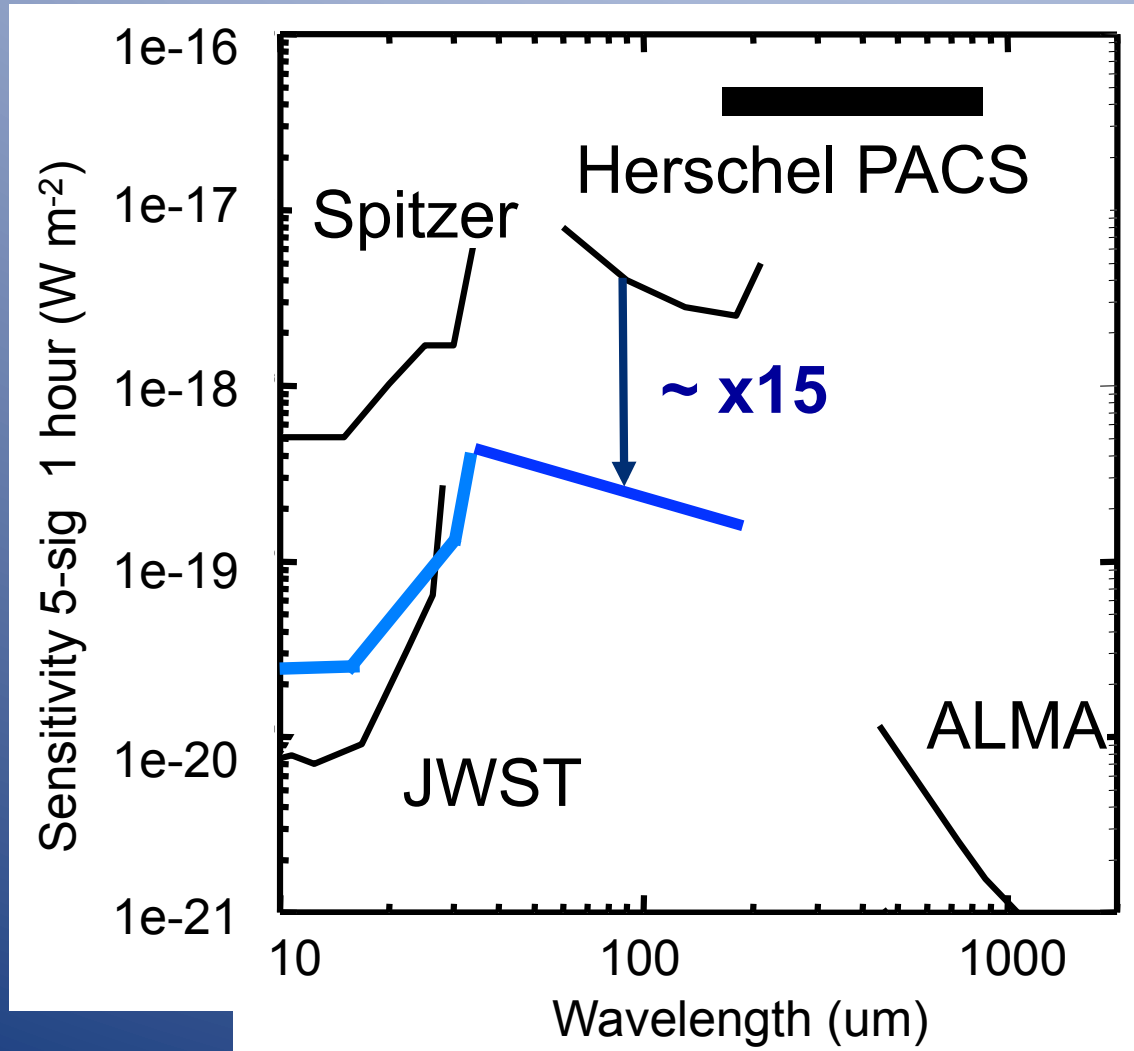
Accretion power in the local universe $z \approx 0.03$:
 $2.1 \cdot 10^{46} \text{ erg/sec}$

SF power in the Seyfert galaxies in the local universe: $2.3 \cdot 10^{45} \text{ erg/sec}$

As seyfert's are ~10% of the total 12μm sample => total SF power ~ total accretion p.

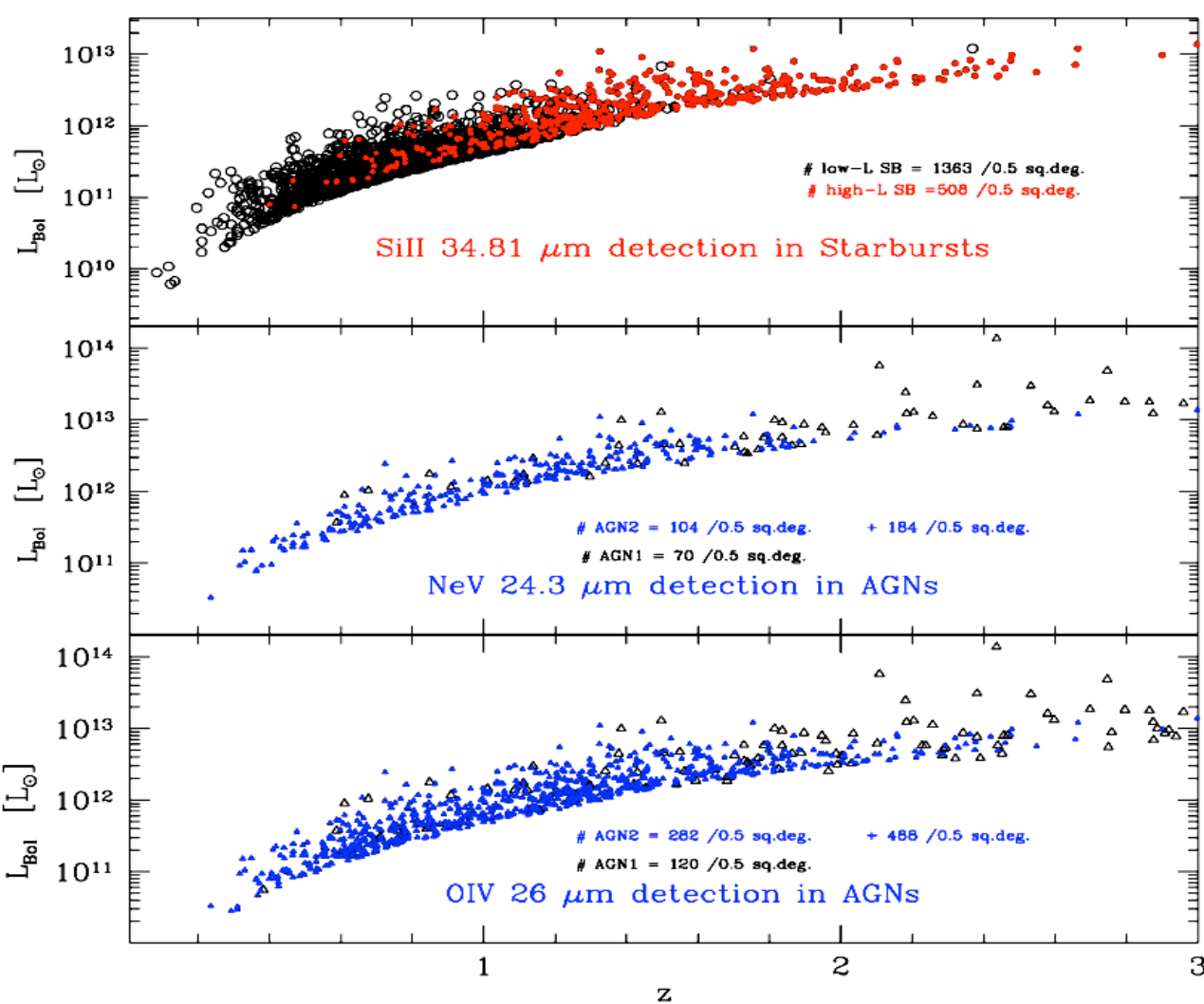
Spinoglio+12

SPICA Sensitivity - spectroscopy



**Single unresolved
line in single
object**

**FTS 100's times
faster to cover
multiple lines over
large field of view**



The figure contains a prediction of the results of a spectroscopic survey over 0.5 square degrees (500 hrs with nominal sensitivity of $2 \times 10^{-19} \text{ W/m}^2 \text{ 1 hr, } 5\sigma$) Numbers of detected sources would be:
 120 Type-1 AGNs [OIV], [NeV]
 770 Type-2 AGNs " "
 1870 starburst galaxies in [SIII] for a total of ~ 2800 objects (Franceschini model)

Gran total of ~ 7 objects per SAFARI field 2' x 2'

Within uncertainties two different models (Gruppioni and Franceschini) predict about 7-10 sources to be spectroscopically detected in more than 1 line down to the expected flux limits of SPICA, with about 20% of sources to be detected at $z > 2$. Similar figures from direct integration of e.g. Magnelli et al. LF

(see Spinoglio+12)

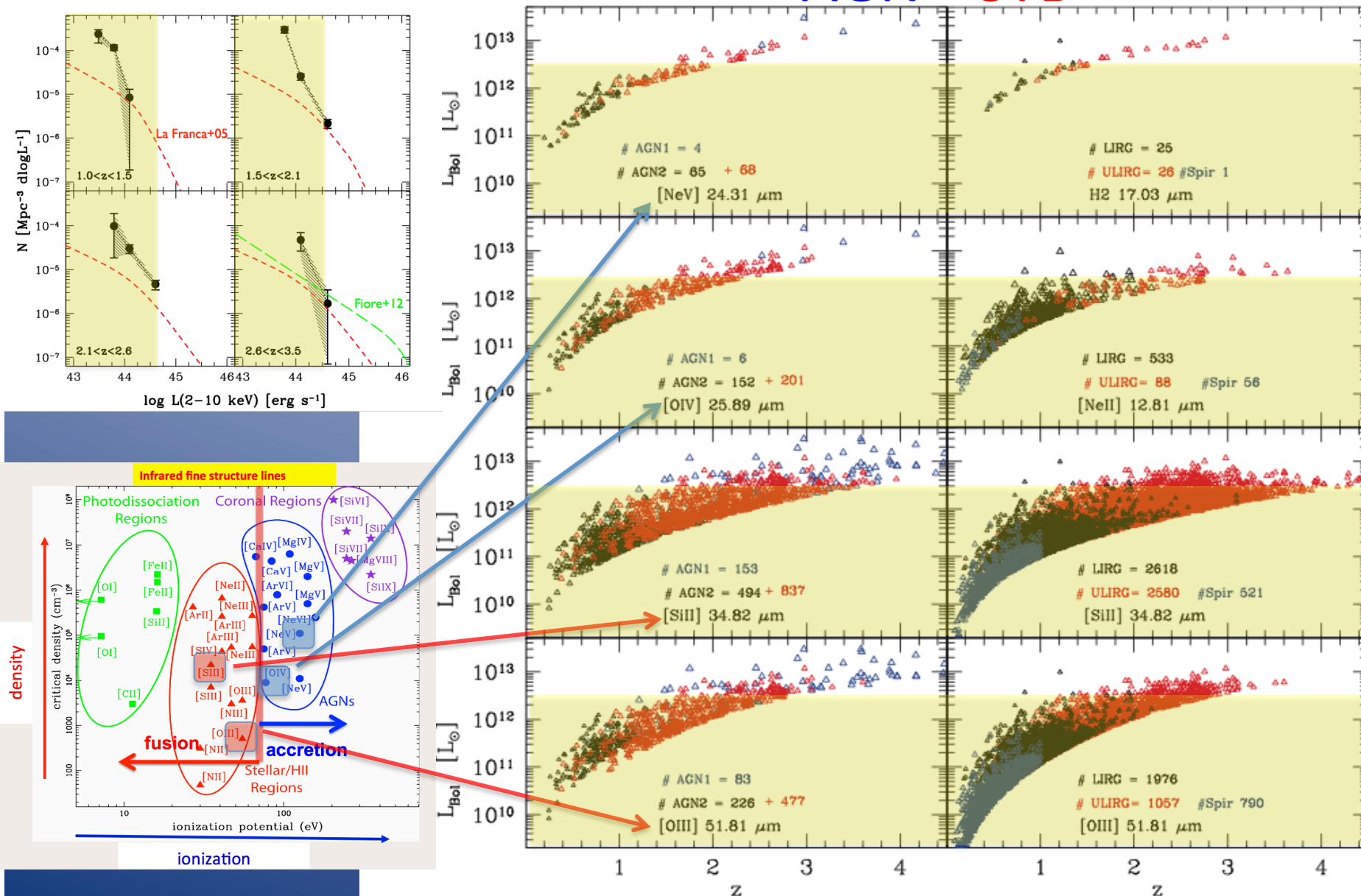


Figure 10. Prediction of the number of sources of a 0.5 deg^2 spectroscopic survey with SAFARI based on Franceschini et al. (2010), giving the number of detectable starburst galaxies (divided by L_{IR}) and AGNs (divided by obscuration) at the 3σ level. The adopted line flux sensitivities as a function of wavelength are given in the Appendix. The left panels correspond to the AGN predictions, the right panels to the starburst predictions. As for the former, the numbers of type 2 AGNs associated with the LIRG and the ULIRG populations are shown separately (in black and red, respectively).